RNA-Catalyzed Amino Acid Activation†

Raju K. Kumar and Michael Yarus*

Department of Molecular, Cellular and Developmental Biology, University of Colorado, Boulder, Colorado 80309-0347

Received April 6, 2001; Revised Manuscript Received May 1, 2001

ABSTRACT: We have selected RNAs that perform a new reaction that chemically activates amino acids, paralleling mixed phosphate anhydride synthesis by protein aminoacyl-transfer RNA synthetases. Care with recovery of the unstable reaction product was apparently essential to this selection. The best characterized RNA, KK13, requires only Ca^{2+} for reaction and is optimally active at low pH with K_M = 50 mM and k_{cat} = 1.1 min^{-1} for activation of leucine. In conjunction with previous RNA-catalyzed aminoacyl-RNA synthesis, peptide bond formation, and RNA-based coding, these amino acid-activating RNAs complete an experimental demonstration that the four fundamental reactions of protein biosynthesis can be RNA-mediated. The appearance of translation in an RNA world is therefore supported.

Modern aminoacyl-tRNA synthetase proteins (aaRS)[1] catalyze two essential translational reactions. The first is the activation of the carboxylate of amino acids by aminoacyl adenylate formation [aa-AMP]. An adenylate is a highly reactive mixed anhydride between the amino acid carboxyl and the α-phosphate of ATP (eq 1). This enzyme-bound adenylate is subsequently used to esterify the 2′(3′) terminus of tRNA (eq 2). A close parallel to eq 2 is carried out by

$$\text{aa} + \text{ATP} \leftrightarrow \text{aa-AMP} + \text{PP}_i \quad (1)$$

$$\text{aa-AMP} + \text{tRNA} \leftrightarrow \text{aa-tRNA} + \text{AMP} \quad (2)$$

RNAs as small as 29 nucleotides (*1*). Using larger RNAs, similar aminoacyl-RNA synthesis is as fast and as specific as by modern aaRS proteins (*2*, *3*). In contrast, RNA catalysis of eq 1, amino acid activation, has been elusive.

The difficulty of this selection might be due to poor nucleophilicity of the carboxyl and/or to product instability (adenylate half-lives are minutes at 0 °C and pH 7). The instability of aminoacyl nucleotides [like aminoacyl-(5′) pRNAs] is greatly increased by the amino acid's α-amino group. However, carboxylic acids instead of amino acids yield a more stable product. In addition, selection at lowered pH (near maximal stability for the desired anhydride) would also conserve the product, once formed. Finally, use of carboxylic acids and low pH together suppresses nucleophilic attack by the α-amino group on the α-phosphate, a possible competing side reaction when amino acid substrates are used. Combining these strategies, we now find many RNAs in randomized oligoribonucleotide pools that form aminoacyl adenylate analogues.

MATERIALS AND METHODS

Selection Procedure. Selection for the activation of carboxylic acids was performed by incubation of a randomized pool of 5′pppRNA transcripts with 3-mercaptopropionic acid (henceforth 3MPA, $HSCH_2CH_2COOH$; Aldrich), a structural analogue of the amino acid cysteine [$HSCH_2CH(NH_2)$-COOH]. We began the selection with gel-purified 121-mer 5′-pppRNA having 2×10^{14} unique sequences with 80 randomized nucleotides. The RNA pool was T7 RNA polymerase transcripts of the DNA template 5′-TGG TCA TGT GAT CGG CGT ATG-N_{80}-TAT CGT GTC ATC GTC GTC C**C**T ATA GTG AGT CGT ATT A-3′, where N implies equimolar use of four deoxynucleotides. The bold-faced underlined C is the transcription start site. The gel-purified 121-nucleotide RNA transcript library was dissolved in 200 mM KCl, 200 mM NaCl, and 50 mM HEPES, pH 7, and heated at 95 °C for 3 min. When the temperature dropped to around 60 °C, a mixture of divalents was added to the final concentrations: 5 mM $MgCl_2$, 5 mM $CaCl_2$, 50 μM $MnCl_2$, and 10 μM $ZnCl_2$; dimethyl sulfoxide (DMSO) and 3-mercaptopropionic acid (3MPA) were added at room temperature to give 2% DMSO and 50 mM 3MPA. Addition of 50 mM 3MPA lowered the overall pH to 4. Incubation was at 25 °C for 18 h. Reactions were stopped by the addition of 50 mM EDTA. The solution was passed through a P30 column (Bio-Rad) in 0.3 M NaOAc at pH 5. Linkage of 3MPA-p-RNA to the thiopropyl group of Sepharose 6B (Pharmacia) was achieved by incubation in binding buffer (50 mM EDTA, 50 mM HEPES, pH 7) for 30 min at room temperature. The matrix was then washed with 1 mL of 1 M NaCl, 5 mM EDTA, and 50 mM HEPES, pH 7, with 3 mL of 1 M NaCl, 5 mM EDTA, 50 mM HEPES, pH 7, and 7 M urea, and finally with water. Disulfide-linked RNAs were then eluted by 100 mM DTT in binding buffer.

After eight cycles of selection−amplification, RNAs able to engage in apparent disulfide formation had increased by

†This work was supported by NIH Research Grant GM 30881 to M.Y.

* To whom correspondence should be addressed. E-mail: yarus@stripe.colorado.edu. Phone: (303)-492-8376. Fax: (303)-492-7744.

[1] Abbreviations: aaRS, aminoacyl-tRNA synthetase; aa-AMP, aminoacyl adenylate anhydride; ATP, adenosine 5′-triphosphate; GTP, guanosine 5′-triphosphate; GMP, guanosine 5′-monophosphate; PP_i, inorganic pyrophosphate; 3MPA, 3-mercaptopropionic acid; DMSO, dimethyl sulfoxide; EDTA, ethylenediaminetetraacetate; HEPES, 4-(2-hydroxyethyl)-1-piperazineethanesulfonic acid; APM, [(*N*-acryloylamino)phenyl]mercuric chloride; Tris, tris(hydroxymethyl)aminomethane; DTT, dithiothreitol; PEI TLC, poly(ethylenimine) thin-layer chromatography.

10.1021/bi010710x CCC: $20.00
Published on Web 05/23/2001

about 120-fold over the background observed in the initial pool (Figure 1). This library was converted to cDNA, cloned, and sequenced (*4*).

Synthesis of [(N-Acryloylamino)phenyl]mercuric Chloride (APM). The monomer (APM) was synthesized by the reaction of (*p*-aminophenyl)mercuric acetate with acryloyl chloride according to a published procedure (*5*).

Preparation of Polyacrylamide Gels Containing APM. For a typical APM gel of 20 cm × 20 cm, 20 mL of a solution containing 8% acrylamide and 7 M urea was combined with 150 μL of a 1 mg/mL solution of APM in formamide. The final concentration was 20 μM APM. To initiate polymerization, 200 μL of 10% ammonium persufate and 20 μL of TEMED were added. Gels were normally prerun in a cold room (4 °C) for 30 min to 1 h before the application of samples and then run for 2 h more. The running buffer was Tris (40 mM)/acetic acid (20 mM)/EDTA (1 mM), pH 6.8.

Reaction Conditions and Activation Assay. Characterization reactions were carried out under optimized conditions; 50 mM substrate (buffered to pH 4), 5 mM Ca^{2+}, and 50 mM NaCl. For the [^{32}P]PP_i release assay, 50 mM cacodylate, pH 4/4.5, was used as buffer control. Internally labeled KK13 pppRNA was prepared by T7 transcription of KK13 PCR DNA in the presence of [α-^{32}P]GTP; internally labeled 5′-OH RNA was prepared by treating pppRNA with shrimp alkaline phosphatase; 5′(^{32}P) RNA was prepared by T4 polynucleotide kinase action on cold 5′-OH RNA. All RNAs were gel purified by 8% denaturing PAGE, eluted, ethanol precipitated, and resuspended in water.

Two activation assays were used. In the first assay, gel-purified KK13 pppRNA was incubated with 50 mM 3MPA for 1 h at 25 °C. The mixed anhydride product, 3MPA-p-RNA, is retarded in 8% denaturing APM−PAGE due to the coordination of thiophilic mercury in the gel matrix with the mercapto group of the mixed anhydride. RNA radioactivity was analyzed by phosphorimaging. In the second assay, used for comparison of amino acids, KK13 RNA labeled at the 5′-γ-phosphate (*pppRNA) was incubated with a 50 mM amount of various amino acids for 2 h at 25 °C, and the reaction mixture was chromatographed with a [^{32}P]PP_i standard using cellulose−PEI TLC with 20% methanol and 80% 0.5 M potassium phosphate at pH 6.3. Released [^{32}P]-PP_i was visualized by phosphorimaging.

Synthesis of Nonisotopic Markers. Synthesis of nonisotopic markers, leucinyl and phenylalanyl guanylate, was carried out by literature methods (*6*). The products were purified by preparative chromatography on C18 cartridges (Waters). To determine that the purified products were anhydrides, not the 2′(3′) esters, the guanylates were individually subjected to periodate treatment and analyzed by HPLC. The quantitative disappearance of the initial peak was observed for both as a result of oxidation of the 2′(3′) diols. Since ester formation would have prevented oxidation, the product was the mixed anhydride between the carboxyl and 5′-phosphate groups. The products were further established by electrospray (+ve) mass spectra: phenylalanyl guanylate (measured = 511, calculated = 510); leucinyl guanylate (measured = 477, calculated = 476).

Kinetic Analysis. Kinetic data for the KK13 RNA reaction with leucine were obtained with ∼1.5 μM RNA incubated with different concentrations of leucine (1−75 mM). Only data generated from 15, 25, 50, and 75 mM leucine were used in the final analysis. Values of k_{obs} were determined by linear regression of released pyrophosphate versus time (after subtracting a parallel pyrophosphate control) using Axum5 (Mathsoft Inc., Cambridge, MA). K_M and k_{cat} were determined, respectively, from the slope and the *y*-intercept of the plot of $1/k_{obs}$ against 1/[leucine].

Identification of Reaction Products by Nuclease P1 Digestion. For HPLC analysis of digestion products, leucine and phenylalanine reacted internally labeled RNAs transcribed in the presence of [α-^{32}P]GTP were ethanol precipitated, and nuclease P1 digests were carried out with 8 units of P1 nuclease (Pharmacia, Sigma) in 10 μL of 10 mM sodium acetate, pH 5, at room temperature for 20 min. Reversed-phase HPLC analysis was carried out by injecting the digested RNA along with nonisotopic synthetic markers. Eluant was collected every 15 s for 20 min and analyzed by scintillation counting. Absorbance at 254 nm was used to localize synthetic nonisotopic markers.

HPLC Analysis. Reversed-phase HPLC analyses of nonisotopic synthetic markers and nuclease P1 digests were carried out using a Varian Microsorb C18 column (25 cm, 5 μm porosity) with buffer A, 0.1 M NH_4OAc, pH 4.5, and buffer B, acetonitrile; a gradient of 50% buffer B in 30 min was used with a flow rate of 1 mL/min.

Secondary Structure. RNA at ∼0.2 μM was heated to 90 °C for 3 min in distilled water. After being cooled to room temperature, NaCl and $CaCl_2$ were added to final concentrations of 50 and 5 mM, respectively. Then NaOAc, pH 4.5, was added to 50 mM. S1 nuclease (GIBCO/BRL) and 50 μM $ZnCl_2$ were now added. Nuclease was 0, 0.025, 0.05, 0.1, and 0.2 unit in a final volume of 10 μL, incubated at room temperature for 20 min. Products were fractionated by using 10% denaturing PAGE with NaOH ladders and T1 RNase digests alongside to identify fragments. Nuclease S1 cuts are shown in Figure 5A.

RESULTS AND DISCUSSION

Selection Design. Selection was for the activation of carboxylic acids. RNAs selected were then assayed for amino acid activation. Activation of the carboxyl group requires nucleophilic attack by the carboxylate on the α-phosphate of 5′pppRNA, leading to the formation of mixed anhydride with concomitant release of inorganic pyrophosphate (Figure 1). The minority of RNAs that reacted with 3MPA was captured on pyridine-activated thiopropyl-Sepharose 6B (*7*, *8*) by forming a disulfide linkage between the sulfhydryl group of 3MPA-p-RNA and the matrix. Immobilized RNAs were recovered by cleaving the disulfide with DTT, ethanol precipitated, and reverse transcribed. These cDNAs were PCR amplified and retranscribed for the next cycle (*4*).

Sequenced Clones. Among 36 sequenced clones, seven repetitively isolated sequences (families) and five unique sequences were identified. Sequences and reactivities with 3MPA are shown in Figure 2. Manual and computed sequence alignment did not reveal any consensus sequence among the different nonclonally derived sequences (Figure 2). That one-third of the reactive sequences are unrelated unique isolates suggests that a large number of different RNAs exist that could meet the selection. RNA KK13 (114 nt) is characterized below. Some reactive RNAs (for example, KK1) form an additional product, possibly a capped

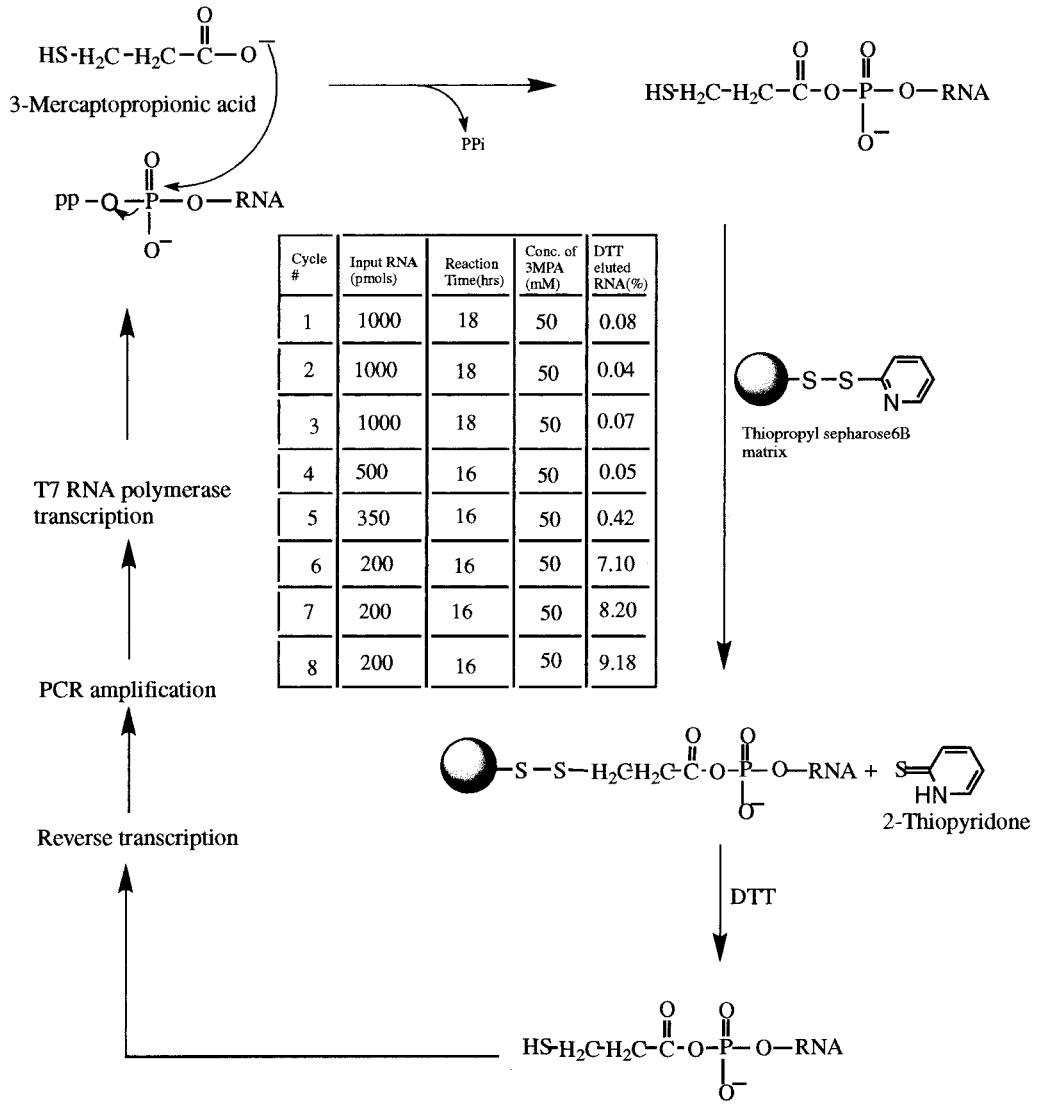

Cycle #	Input RNA (pmols)	Reaction Time(hrs)	Conc. of 3MPA (mM)	DTT eluted RNA(%)
1	1000	18	50	0.08
2	1000	18	50	0.04
3	1000	18	50	0.07
4	500	16	50	0.05
5	350	16	50	0.42
6	200	16	50	7.10
7	200	16	50	8.20
8	200	16	50	9.18

FIGURE 1: Selection protocol for carboxyl-activating ribozymes. Active RNAs are covalently linked to pyridine-activated thiopropyl-Sepharose 6B and subsequently eluted with DTT. Table: Enrichment of carboxyl-activating RNA versus selection cycle.

5′−5′ dimeric RNA of divergent polarity. Such RNAs result from attack of the γ-phosphate of one RNA on the α-phosphate of another (data not shown). KK13 gives bona fide carboxyl activation as its only RNA product (vide infra). Hence, detailed studies were carried out with KK13 around its optimum pH of 4−4.5.

Determination of the Reaction Center. Activation of the carboxyl group (3MPA/amino acids) requires the nucleophilic attack of carboxylate oxygen on the 5′-α-phosphate of RNA, releasing PP_i (Figure 1). Thus product formation should require a 5′-terminal triphosphate. In support of this prediction, no reaction was observed for 5′-pRNA and 5′-OH RNA tested by APM gel electrophoresis (Figure 3A) (*5*). In this assay, sulfhydryl-bearing RNAs move slowly through the gel matrix due to interaction with thiophilic mercury in the APM, which is a covalent subunit of the polyacrylamide matrix (*5*, *8*, *9*). RNA was incubated with 3MPA, freed of 3MPA by gel filtration, and loaded onto 8% denaturing APM−PAGE. In Figure 3A, only 5′pppRNA yielded a slow-moving product, consistent with reaction at the RNA's 5′-α-phosphate.

APM gel electrophoresis also shows that the carboxyl group of the small molecule substrate is required. Experiments using RNA incubated with cysteamine (amino replacing the carboxyl of 3MPA) and propanethiol (a methyl group in the place of carboxyl) yielded no product on the APM gel (Figure 3B). Thus, the carboxyl is the nucleophile. This conclusion was further substantiated by measurement of [^{32}P]-PP_i release, which showed substrate-dependent evolution of pyrophosphate for 3MPA but not for cysteamine and propanethiol (data not shown).

Such pyrophosphate release generally corroborates the predicted reaction center. Activation of amino acids was assayed by incubating RNA KK13 [labeled at the 5′-γ-phosphate (*pppRNA) by transcription in the presence of [γ-^{32}P]GTP] with 50 mM amino acids for 2 h at 25 °C, and the reaction mixture was compared to *PP_i standards using cellulose−PEI TLC and phosphorimaging (Figure 3C).

RNA KK13 shows 5′-pyrophosphatase (attack by water) as well as the activation activity (attack by carboxyl). However, in Figure 3C, the substrate-dependent reaction of RNA KK13 was easily detectable: pyrophosphate release was stimulated almost 3-fold in the presence of varied amino acids. Therefore, the reaction center for amino acid activation as well as pyrophosphatase is the 5′-α-phosphate, but amino

Number of Sequences in family	Clone #	Family/Sequence	Retarded on APM Gel (%)
3	13	CAUGAGAGACAUAUGAUUCGUGAUGGGAGUCACUGGCGCAGUGGUGCCGGAAAUCCAACUACUUCUGAGGGGA	21.5
6	1	AGUAGGCCGCGCAUCACACGUAGGCAUAAUACUGCGCAUUGCGAAAGGAGGCCACAGUCGUCAUCAGAGUGAAGCCAGGG	17.1
2	10	ACAUAGGCAGGAAGCCUCAGUCAGGUUUCUAAGAUGCGGCCAUUGCAGUCAUCAACGGUUAUGAAUCGAGCCAUAGUUUG	11
1	4	GGCGUCAGGAGGUGUGCAGAGACCUCCAAUAAGCAUCCCUGCGGCCAGGUCUACAACAUAAUCUGGACGAGGAAGACG	5.9
3	26	CUGCGUCUGCACGCAAACUGUGGUGGCGCGGGCAUGCCAGAAUUGUCAGGUUCAACAAGAUAAUUAGCGAUGGGAA	5.1
1	20	AACGUGCGCCCAUGGCGGACGUUGUGAUACAUUUGGUCAGGUACAACAAUAGGUUGACCGUAUGUGGGAG	3.5
4	15 27 19-1 32	AAAGGACAUGUAAUUUCCCAUAAGUAUACGGGUGUGUGUUGAAGAUAUGUCCUGGGGGCUCAUAGAAUGGCCAUCAGCUG C----------G---------- C----------C----------A C----------C----------	Not Reactive
3	19-2	UAGCGAUCAAGAGGCGCUGCGCGUCUGGAGUUUCCGCAAAAAAGAGUUAUGUUGGUGAAGCCAGACGAGGCUAGGAAUGA	Not Reactive
2	3	UUAGACUUAGAGAUUCCCAGUGGAGGUAACAGAUUAGGGACCUAGGGGGAAAUGUGUUGUAGCUAAGUUGCAAGUGGUU	Not Reactive
1	33-1	GAAUGUGCAUGGAUAUCGUCAGGAGCAACAAUAUAAUUGACGGAUAUAGCGGUACGCAAAAUCGACACGAGUU	Not Assayed
1	33-2	GGGUUGCGGGCUAGAAGCAACGAGGUACUAAUUAAUUUCCUUUUAACUGGUCGAGUUGAAGAAUUACGAAAUGUAGUGG	Not Assayed
1	35	CGGCAAGGGGCUAACUCCAUGUUAACAUGUAGUGGUUGGAAGUGUUUUGUCGUCAGGUGCUACAAUAUCAUCGGAGCUU	Not Assayed

FIGURE 2: Randomized regions of sequences obtained from selection; the flanking 5′-end and 3′-end constant sequences are, respectively, 5′-GGG ACG ACG AUG ACA CGA UA-3′ and 5′-CAU ACG CCG AUC ACA UGA CCA-3′. Left: number of sequences in a family, followed by representative sequence number(s). Right: reactivities as a percentage of the total RNA retarded on the APM gel after incubation in 50 mM 3MPA for 1 h.

acid activation is the predominant reaction under these conditions.

Substrate-dependent [^{32}P]PP$_i$ RNA exchange activity was also observed for the RNA KK13 reaction with 3MPA and amino acids, as for the original detection of protein aaRSs (*10*; data not shown). Formation of a mixed anhydride would promote [^{32}P]PP$_i$ exchange via a reverse reaction:

$$\text{R}-\text{C(O)}-\text{O}-\text{pRNA} + [^{32}\text{P}]\text{PP}_i \rightarrow \text{R}-\text{C(O)}-\text{O}^- + {}^{32}\text{pppRNA}$$

Substrate stimulation of [^{32}P]PP$_i$ exchange supports the formation of a reactive first product (the anhydride), which re-reacts readily with free isotopic pyrophosphate to label the catalytic RNA with [^{32}P]PP$_i$.

Therefore, the amino acid carboxyl reacts at the 5′-α-phosphate of 5′pppRNA KK13 to release PP$_i$ and make an activated product, amino acid guanylate. We now show that substrates leucine and phenylalanine generate the corresponding bona fide activated amino acids.

HPLC Analysis of the Activation Reaction Products (Leucinyl and Phenylalanyl Guanylates). Product characterization for 5′-aminoacyl-p-RNA KK13 uniformly labeled with [α-^{32}P]GTP exploited nuclease P1 digestion products resolved on HPLC. Nuclease P1 digestion (which normally releases 5′ nucleotides) of 5′-aminoacyl RNA yields amino acid GMP (from the reacted 5′ RNA termini), GTP (from unreacted 5′ RNA termini), and GMP (from internal positions). Products were established by HPLC cochromatography with authentic nonisotopic molecular markers. Radioactivity of 5′-terminal guanylates from KK13 RNA precisely tracked the absorbance of authentic leucinyl guanylate and phenylalanyl guanylate during reversed-phase HPLC (Figure 4). This experiment was also done with 3MPA (not shown). Comigration of three RNA products with three different synthetic mixed anhydrides persuasively establishes the identity of the activation product.

Secondary Structure of KK13 RNA. A stable secondary structure calculated for RNA KK13 (Figure 5A) is in reasonable agreement with nuclease S1 accessibility data, save that the helix on the left may not be fully formed. This approximate secondary structure model suggests that the active site may be principally formed by enveloping the 5′-triphosphate in a structured loop.

Michaelis−Menten Kinetics. Apparent first-order rates for leucine reaction with KK13 at pH 4 and 4.5 were obtained by fitting the released [^{32}P]PP$_i$ over time. Analysis to derive K_M and k_{cat} (Figure 5B) could not be carried above 75 mM due to the limited solubility of leucine and could not be extended below 15 mM because PP$_i$ release was then dominated by pyrophosphatase activity. Net pyrophosphate

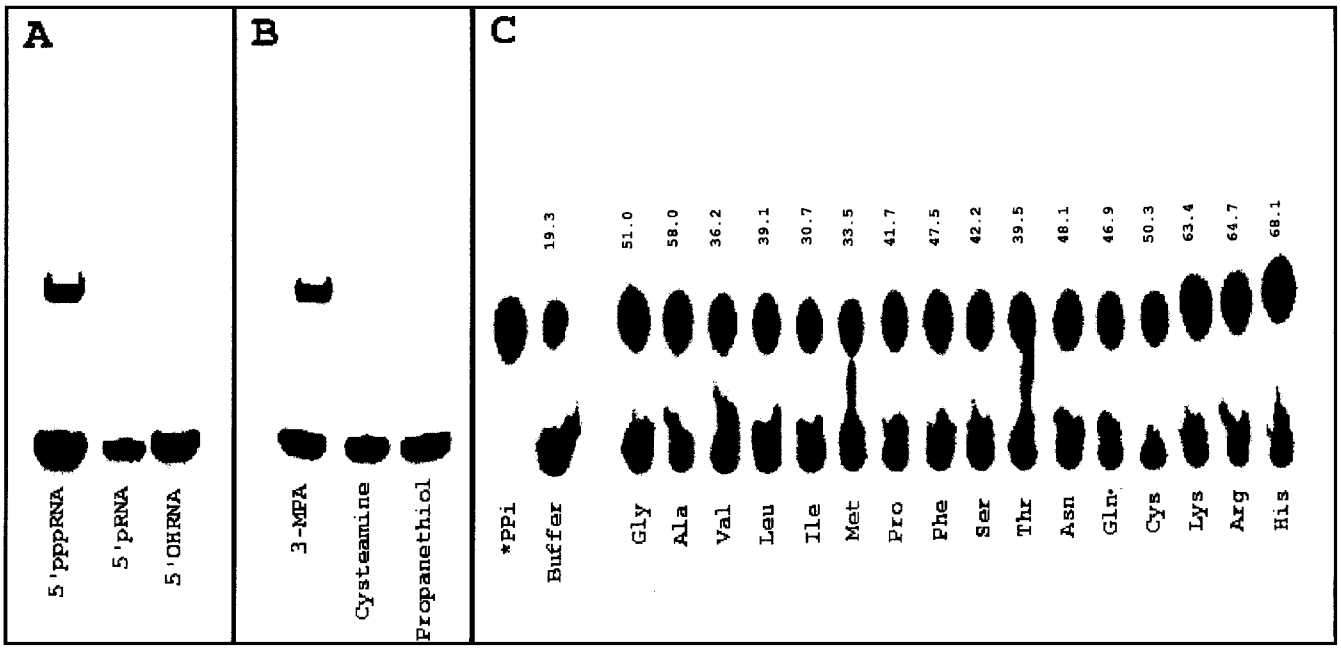

FIGURE 3: (A) APM gel assay [8% acrylamide, 7 M urea, and 20 μM (acryloylaminophenyl)mercury] showing the requirement for 5′-triphosphate RNA for activation of the 3MPA carboxyl group (lane 1). Lanes 2 and 3 for 5′-pRNA and 5′-OH RNA, respectively, did not show any retarded band. (B) Requirement for a carboxyl group for nucleophilic attack on the α-phosphate of 5′-triphosphate RNA (lane 1). Cysteamine (lane 2) and propanethiol (lane 3) are not substrates for the RNA. (C) TLC analysis of the pyrophosphate release for the reaction of amino acids with 5′-γ-^{32}P-labeled KK13 (^{32}pppRNA) for 120 min at room temperature in cacodylate buffer, pH 4. Numbers show the percent of released pyrophosphate.

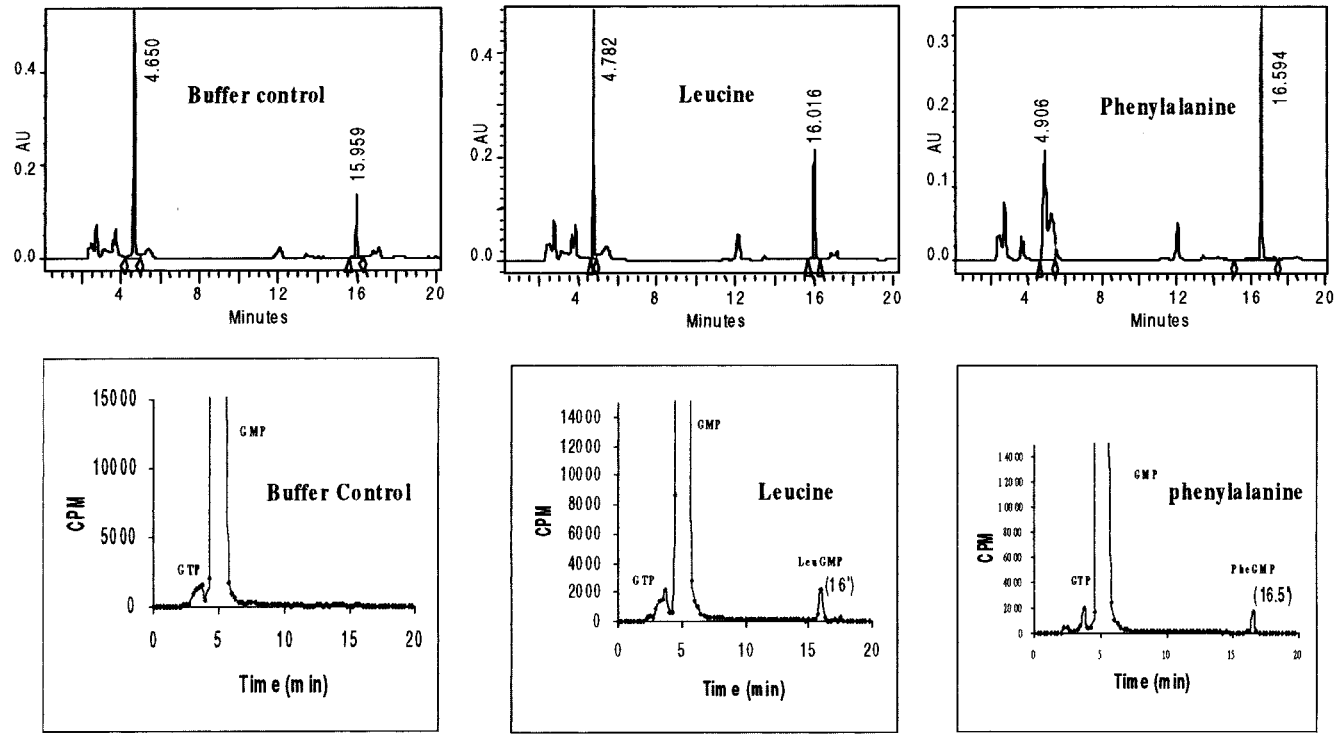

FIGURE 4: Analysis of nuclease P1 digestion products from leucinyl-p-RNA and phenylalanyl-p-RNA by HPLC in acetonitrile−0.1 M NH_4OAc gradient, C18 column. Top: HPLC trace (absorbance at 254 nm) of the respective analyte. The added marker in the buffer control was leucinyl guanylate; Bottom: Plot of CPM against time, tracing the peak of leucinyl guanylate (LeuGMP) and phenylalanyl guanylate (PheGMP) to the retention time of cold activated amino acid markers.

release data from the accessible range are acceptably Michaelis−Menten with $k_{cat} = 1.1$ min $^{-1}$ and $K_M = 48.1$ mM at pH 4. The corresponding values at pH 4.5 are 0.2 min^{-1} and 30.0 mM. Thus k_{cat}/K_M is 3-fold lower at pH 4.5 than at pH 4. The observed K_M is notably close to 3MPA substrate levels during selection (50 mM).

Conditions for Activation of the Carboxyl Group. The full complement of divalents used in selection was not required for reaction, which needs only buffered calcium. Without calcium there is no observable reaction. Monovalents could be omitted, although a final concentration of 50 mM NaCl was slightly stimulatory. The active catalyst may therefore

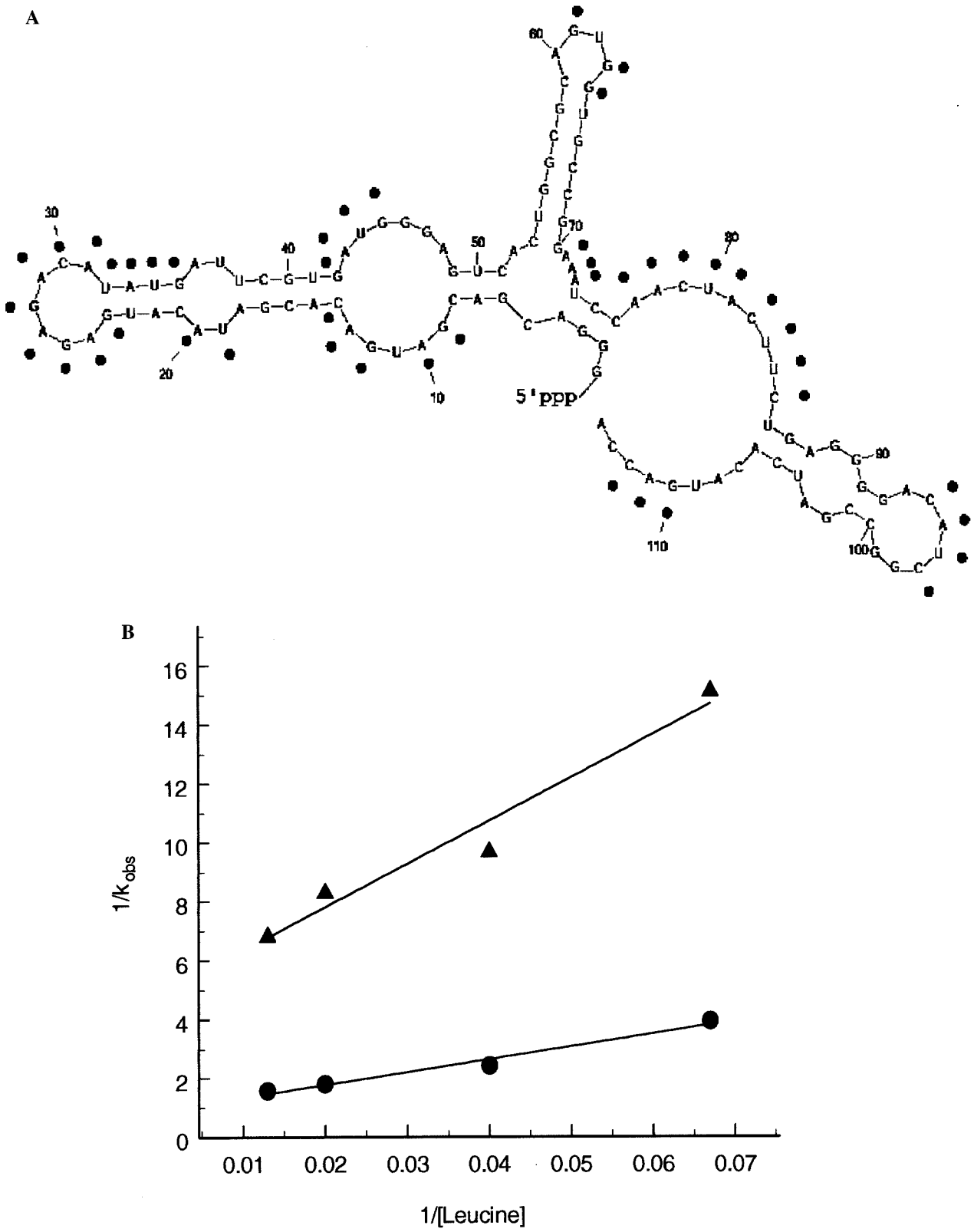

FIGURE 5: (A) Secondary structure of KK13 RNA predicted by Mfold and confirmed by nuclease S1 probing. Faster S1 scissions are indicated by filled circles. (B) Fit of net rate data versus the concentration of leucine (filled circles for pH 4 and filled triangles for pH 4.5).

be a Ca^{2+}-RNA. Such an exclusive requirement for Ca^{2+} in RNA catalysis has earlier been observed for the 5′-RNA self-capping ribozyme (*11*, *12*), and a special role for Ca^{2+} has also been shown for self-aminoacylating RNA (*13*). Activation of a carboxyl group by RNA brings a negatively charged nucleophile and a negatively charged phosphate together. This might occur via a calcium−phosphate chelate. The idea that special reactivities will be associated with special divalent−RNA structures, termed the Cheshire Cat conjecture (*14*), seems to be well exemplified by Ca^{2+}-RNA.

This ribozyme functions best at pH 4−4.5; and indeed function at such pH was required by the selection and may have been essential to its success. There are two prior RNAs selected in vitro requiring mildly acid pH, similar to KK13

RNA; one is a self-cleaving ribozyme (*15*) and the other an aptamer recognizing coenzyme A (*16*). We will now try to shift the operational pH of RNA KK13 upward or, alternatively and perhaps more straightforwardly, try to increase the reaction rate at low pH. A more reactive KK13-like domain can be conjoined to an aminoacyl-RNA synthesis domain (*3*) to (re)constitute an RNA aaRS that works near neutrality. However, the pH response of RNA-catalyzed aa-RNA synthesis is well characterized (*3*); thus even already known RNA domains could likely be combined to yield aaRS activity at pH 5−6.

Conclusions. There are several notable implications of this new selection. First, carboxyl oxygen attack on phosphorus represents new ribozyme chemistry. RNA KK13 activates carboxyl groups in many chemical contexts and thereby potentially makes accessible a new set of reactions important in biochemistry and organic chemistry. These ribozymes, for example, may be usable for the activation of fatty acids for synthesis of acyl-CoA's.

However, a translational motive drove the selection for this ribozyme. The RNA world hypothesis predicts a biota before the appearance of coded peptide synthesis. For these ancestral creatures, most biological catalysts were RNA or a closely related molecule (*17*). The notion of immediate succession from such RNA organisms to the present biota, with its dominant protein catalysts, then necessarily predicts that RNA catalysts were the first to perform protein biosynthesis. Thus RNA catalysts that activate amino acids, synthesize aminoacyl-RNA, and form peptide bonds are almost inevitably predicted. In addition, RNAs must originate coding.

Remarkably, with the discovery of RNA-catalyzed amino acid activation by RNA KK13, all four predicted reactions have been observed. RNA KK13 activates amino acids by forming aminoacyl guanylates. These are chemically similar to aminoacyl adenylates, the universal modern step toward translational reactivity. The second reaction, transfer of activated amino acids to the 2′(3′) terminus of an acceptor RNA, is an easy RNA-catalyzed reaction. It can be catalyzed by small RNAs (*1*, *18*) and can be done rapidly and with high amino acid side chain specificity (*3*). For the third reaction, peptidyl transferase, RNA synthesis of amides was first shown by modification of RNA catalysts selected for ester formation within a template helix (*19*) and then for modified imidazole-U RNA without templating (*20*). Peptide bond forming ribozymes can, however, be isolated directly from pools of randomized RNAs (*21*). Moreover, a transition state analogue for the ribosomal peptidyl transferase, CCdAp-Puro (*22*), has been used to localize the biological peptidyl transferase in the large ribosomal subunit (*23*). Because of the absence of peptide within a protein's diameter of this active site, it appears that peptidyl transfer is still an RNA reaction (*24*). The direct selection of most of the peptidyl transferase reaction center from randomized RNAs, using affinity to the transition state analogue CCdApPuro (*22*), suggests that peptidyl transferase may be very much as it was in an RNA world (*24*). Fourth, there is substantial evidence that some modern codons are derived from triplet sequences in ancient amino acid binding sites for their cognate amino acids (*25*).

Thus we can jointly confirm the four predicted RNA-mediated translational reactions with laboratory examples. Each of the four is nontrivial even when taken by itself. Accordingly, the joint existence of these four RNA reactions is very unlikely to be accidental. Said another way, the required exit from an RNA world existed. Accordingly, the RNA world itself likely existed in some form.

ACKNOWLEDGMENT

We thank Mali Illangasekare, Vasant Jadhav, Irene Majerfeld, Mark Robida, Alexandre Vlassov, and Ico de Zwart for comments on a draft manuscript.

REFERENCES

1. Illangasekare, M., and Yarus, M. (1999) *RNA 5*, 1482.
2. Illangasekare, M., Sanchez, G., Nickles, T., and Yarus, M. (1995) *Science 267*, 643.
3. Illangasekare, M., and Yarus, M. (1999) *Proc. Natl. Acad. Sci. U.S.A. 96*, 5470.
4. Ciesiolka, J., Illangasekare, M., Majerfeld, I., Nickles, T., Welch, M., Yarus, M., and Zinnen, S. (1996) *Methods Enzymol. 267*, 315.
5. Igloi, G. L. (1988) *Biochemistry 27*, 3842.
6. Berg, P. (1958) *J. Biol. Chem. 233*, 608.
7. Lorsch, J. R., and Szostak, J. W. (1994) *Nature 371*, 31.
8. Wecker, M., Smith, D., and Gold, L. (1996) *RNA 2*, 982.
9. Unrau, P. J., and Bartel, D. P. (1998) *Nature 395*, 260.
10. Berg, P. (1956) *J. Biol. Chem. 222*, 1025.
11. Huang, F., and Yarus, M. (1997) *Biochemistry 36*, 6557.
12. Huang, F., and Yarus, M. (1998) *J. Mol. Biol. 284*, 255.
13. Illangasekare, M., Kovalchuke, O., and Yarus, M. (1997) *J. Mol. Biol. 274*, 519.
14. Yarus, M. (1993) *FASEB J. 7*, 31.
15. Jayasena, V. K., and Gold, L. (1997) *Proc. Natl. Acad. Sci. U.S.A. 94*, 10612.
16. Burke, D. H., and Hoffman, D. C. (1998) *Biochemistry 37*, 4653.
17. White, H. B., III (1976) *J. Mol. Evol. 7*, 101.
18. Lee, N., Bessho, Y., Wei, K., Szostak, J. W., and Suga, H. (2000) *Nat. Struct. Biol. 7*, 28.
19. Lohse, P. A., and Szostak, J. W. (1996) *Nature 381*, 442.
20. Wiegand, T. W., Janssen, R. C., and Eaton, B. E. (1997) *Chem. Biol. 4*, 675.
21. Zhang, B., and Cech, T. R. (1997) *Nature 390*, 96.
22. Welch, M., Chastang, J., and Yarus, M. (1995) *Biochemistry 34*, 385.
23. Nissen, P., Hansen, J., Ban, N., Moore, P. B., and Steitz, T. A. (2000) *Science 289*, 920.
24. Yarus, M., and Welch, M. (2000) *Chem. Biol. 7*, R187.
25. Yarus, M. (2000) *RNA 6*, 475.

BI010710X